Optical and Quantum Electronics **27** *(1995) 1397–1406*

Metal surface temperature induced by moving laser beams

G. R. B. E. RÖMER, J. MEIJER
University of Twente, Department of Mechanical Engineering, Laboratory of Mechanical Automation, PO Box 217, 7500 AE Enschede, The Netherlands

Received 27 October 1994; accepted 21 March 1995

Whenever a metal is irradiated with a laser beam, electromagnetic energy is transformed into heat in a thin surface layer. The maximum surface temperature is the most important quantity which determines the processing result. Expressions for this maximum temperature are provided by the literature for stationary cases. In practice, however, moving beams are of more importance.

Based on a fast numerical algorithm which allows calculation of the induced temperature profile, the maximum surface temperature for stationary and moving laser beams is calculated. Next, two types of approximating functions are presented relating the scanning speed to the maximum surface temperature. Using dimensionless numbers, the results can be applied to different materials.

1. Introduction

Laser surface treatment is a promising technique for improving wear and fatigue resistance of machine components on a local basis [1]. The improvement is based on rapid thermal cycling of the surface layer, resulting in microstructural refinement, phase transformation or formation of supersaturated solid solutions. First, the material is rapidly heated by absorption of laser radiation. After heating, the material will be self-quenched by the conduction of heat into the bulk material.

Two classes of laser surface treatment can be distinguished: thermal processes, which involve changes of the microstructure of the surface layer, such as hardening and remelting; and thermochemical processes, which includes all processes which change the surface composition by addition of new materials, such as alloying and cladding.

For transformation hardening it has been found that harder surface layer structures and lower stresses are obtained at higher surface temperatures [2]. Hence, the maximum surface temperature is an important quantity determining the processing result and should be controlled on-line.

Thermal models are used to analyse surface temperature profile as a function of the process parameters. For stationary situations, analytical models for the maximum surface temperature induced by several typical laser beams are available from the literature [3]. In practice, however, situations of moving beams are of more importance. Unfortunately, only a few analytical thermal models for moving laser beams which are relevant in surface processing are available. Numerical models are time-consuming, which excludes these algorithms from being used in a laser temperature control setup. Based on a fast numerical algorithm, *multigrid multilevel*

0306–8919

integration [4], two types of functions are proposed which approximate the actual maximum surface temperature induced by moving laser beams.

The results are presented in dimensionless numbers, which implies that the results can be applied easily to different materials, velocities and dimensions.

This paper is organized as follows. In Section 2 some preliminaries are discussed. In Section 3 analytical models of the maximum surface temperature induced by stationary laser beams are enumerated. In Section 4 the maximum surface temperature induced by moving laser beams is discussed. In Section 5 the theory is compared with experimentally obtained results. Finally, Section 6 presents the conclusions.

2. Preliminaries

2.1. Coordinate system

In Fig. 1, the coordinate system and the relative velocity v of an arbitrary laser beam with respect to the metal surface are defined.

2.2. Peclét number

In the literature there is some confusion concerning the definition of the Peclét number, i.e. the ratio between the bulk heat transfer and the conductive heat transfer. Here the Peclét number is defined as

$$P_n \equiv \frac{2av}{\kappa} \tag{1}$$

where κ is the heat diffusivity of the irradiated material and a is half the maximum length of the laser spot in the direction of the velocity (Fig. 2).

The Peclét number will also be referred to as the *dimensionless velocity* $\bar{v}$.

2.3. Nomenclature

P	absorbed laser power (W)
$I(x, y)$	absorbed power density ($W\,m^{-2}$)
P_n	($\equiv \bar{v}$) Peclét number (dimensionless)
$T(x, y)$	steady-state surface temperature profile (K)
v	relative velocity ($m\,s^{-1}$)
x	coordinate in direction of velocity (m)

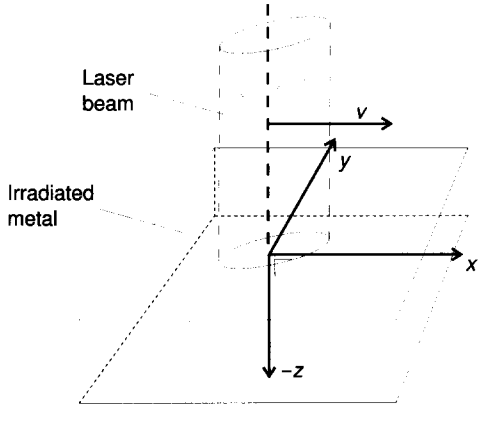

Figure 1 Definition of coordinate system and relative velocity v.

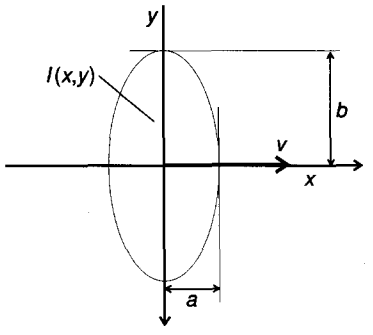

Figure 2 Definition of an arbitrary laser spot intensity $I(x,y)$ on the surface of the body and the characteristic lengths a and b.

y	coordinate perpendicular to velocity (m)
a	laser spot width (m)
b	laser spot length (m)
Φ	(b/a) laser spot aspect ratio (dimensionless)
t	time (s)
c_p	specific heat ($J\,K^{-1}\,kg^{-1}$)
λ	heat conductivity ($W\,m^{-1}\,K^{-1}$)
κ	$(\lambda/\rho c_p)$ heat diffusivity ($m^2\,s^{-1}$)

Remarks

(i) All temperatures T presented in this paper represent a temperature *increase* relative to the initial temperature of the irradiated body.

(ii) Although the thermal parameters, such as specific heat c_p and heat conductivity λ vary with the temperature and hence with the position in the material, here these parameters are assumed to be constant. In the models presented here, average values are taken of the parameters corresponding to the temperature cycle. Such *effective* parameters [5] proved to be adequate. The results are comparable to the results obtained with finite difference models [6] in which the real temperature dependence is taken into account.

(iii) The surface absorptivity of the laser radiation is assumed to be constant.

(iv) The latent heat of the phase transformation and heat losses through the surface are negligible compared to the other terms in the heat-flow equations [19].

3. Surface temperature induced by stationary beams

Some relevant analytical models for the maximum surface temperature from the literature are summarized. It is assumed that the laser energy is transformed into heat in a very thin surface layer, which is the case for metals.

3.1. Circle having uniform intensity and radius R

Consider a circular laser spot with radius R having a uniform power distribution; this is sometimes referred to as a *top hat* distribution:

$$I_{TH}(x,y) = \begin{cases} I_0 & \sqrt{x^2+y^2} \le R \\ 0 & \sqrt{x^2+y^2} > R \end{cases} \tag{2}$$

where $I_0 = P/(\pi R^2)$ is constant. The maximum steady-state temperature at the metal surface in the centre of the laser spot equals [7]

$$T_{\mathrm{TH}}(0,0) = \frac{I_0 R}{\lambda} = \frac{P}{\pi R \lambda} \tag{3}$$

3.2. Gaussian distribution having 1/e radius R_1

The power distribution of a laser beam operating in TEM_{00} mode is described by a Gaussian distribution,

$$I_{\mathrm{G}}(x,y) = I_0 \, \mathrm{e}^{-(x^2+y^2)/R_1^2} \, \forall \, (x,y) \tag{4}$$

where R_1 is the radius at which the intensity $I_{\mathrm{G}}(x,y)$ is reduced by a factor 1/e compared to the maximum intensity $I_0 = P/(\pi R_1^2)$. The maximum steady-state temperature at the irradiated surface in the centre of the spot equals [8]

$$T_{\mathrm{G}}(0,0) = \frac{I_0 R_1}{\lambda} \sqrt{\frac{\pi}{4}} \tag{5}$$

3.3. Rectangle having uniform intensity

For laser surface processing, a rectangular beam shape with a uniform power distribution is preferred [1]. The maximum steady-state temperature at the irradiated surface in the centre of the spot, bounded by $-\frac{1}{2}l < x, < \frac{1}{2}l$ and $-\frac{1}{2}b < y < \frac{1}{2}b$, equals [3]

$$T_{\mathrm{R}}(0,0) = \frac{P}{\lambda \pi l b} \left[b \sinh^{-1}\left(\frac{l}{b}\right) + l \sinh^{-1}\left(\frac{b}{l}\right) \right] \tag{6}$$

4. Surface temperature induced by moving laser beams

Numerical algorithms are usually used to obtain the surface temperature induced by moving laser beams.

4.1. Multigrid multilevel integration

The numerical approach to calculating maximum surface temperature induced by a moving laser beam is based on the numerical solution of the heat equation for a heat point-source moving over the surface of a semi-infinite solid, followed by an integration over the area S of the heat source [7]. The steady-state surface temperature profile of a semi-infinite solid, induced by a moving laser beam with an arbitrary power distribution, written in dimensionless variables, can be expressed as [9]

$$\bar{T}(\bar{x},\bar{y}) = \frac{1}{2\sqrt{\phi}} \int\int_S \frac{\bar{I}(\chi,\gamma) \, \mathrm{e}^{-P_{\mathrm{n}}[r-(\bar{x}-\chi)]}}{r} \, \partial\chi \, \partial\gamma \tag{7}$$

where

$$r = \sqrt{(\bar{x}-\chi)^2 + (\bar{y}-\gamma)^2} \tag{8}$$

with dimensionless variables $\bar{x} = x/a$, $\bar{y} = y/a$, $\bar{I} = I(ab/P)$ and $\bar{T} = T(\lambda\pi\sqrt{ab}/P)$ (see also Fig. 2).

By approximating the laser spot power density as piecewise constant with the value

$\bar{I}_{k,l} = \bar{I}(\chi_k, \gamma_l)$ in the region

$$\{(\chi, \gamma) \in \mathcal{R}^2 | \chi_k - h/2 \leq \chi \leq \chi_k + h/2 \wedge \gamma_l - h/2 \leq \gamma \leq \gamma_l + h/2\}$$

on a uniform grid of mesh size h, the temperature in grid point (i, j) with $(\bar{x}_i = \bar{x}_0 + ih$, $\bar{y}_l = \bar{y}_0 + jh)$ can be written as [9]

$$\bar{T}(\bar{x}_i, \bar{y}_j) = \frac{1}{2} \frac{1}{\sqrt{\Phi}} \sum_{k=0}^{n_x} \sum_{l=0}^{n_y} K_{ijkl} \bar{I}_{k,l} \tag{9}$$

where the coefficients K_{ijkl} are given by

$$K_{ijkl} \equiv \int_{x_m}^{x_s} \int_{y_m}^{y_s} \frac{\mathrm{d}u\, \mathrm{d}w}{\sqrt{u^2 + w^2}} \, \mathrm{e}^{-P_n \left[\sqrt{u^2 + w^2} - u\right]} \tag{10}$$

with

$$u = \bar{x} - \chi, \qquad x_s = \bar{x}_i - \chi_k + h/2, \qquad x_m = \bar{x}_i - \chi_k - h/2,$$

$$w = \bar{y} - \gamma, \qquad y_s = \bar{y}_i - \gamma_l + h/2, \qquad y_m = \bar{y}_i - \gamma_l - h/2$$

Equation 9 represents a straightforward method for calculating the surface temperature numerically, and is generally referred to as the *multi-integration* method. From a computational point of view, the evaluation of Equation 9 is inefficient as it requires $O(N^2)$ operations, N being the number of nodes on a grid. An algorithm, referred to as *multilevel multi-integration* [4], evaluates expressions such as Equation 9 in only $O(N \log(N))$ operations.

Expressions 7 to 10 can easily be extended to include the z-direction. Then the temperature profile *in* the material can be calculated and the induced microstructural changes can be predicted [5].

Besides theoretical power densities, measured power densities can also be used as input, yielding a powerful tool for the analysis of the thermal effects of a specific laser beam.

4.2. Numerical results

The surface temperature profiles resulting from different moving laser spot geometries are shown in Fig. 3.

From this figure the effect of the spot geometry and velocity ($\bar{v} \neq 0$) on the temperature profile is clearly visible. In the case of no velocity ($\bar{v} \neq 0$), the temperature profiles would be symmetric along the x-axis.

Compared to stationary laser beams, for moving beams the position of the maximum temperature shifts from the centre of the spot to the negative x-direction. This should be taken into account when the maximum surface temperature is measured during surface treatment.

In Fig. 4 the maximum dimensionless surface temperature $\bar{T} = \max\{\bar{T}(\bar{x}_i, \bar{y}_j)\}$ is given as a function of the dimensionless velocity $\bar{v}$, for several laser spot geometries with constant power P and constant size a (Fig. 2). It is clearly shown that the maximum surface temperature decreases with increasing feed rate. The top hat power density induces the highest surface temperature for all velocities. The maximum surface temperature of the rectangular laser spots decreases with increasing spot aspect ratio Φ.

As is to be expected, for decreasing velocities ($v \to 0$) the curves in Fig. 4 converge to the dimensionless equivalents of the temperatures enumerated in Section 3.

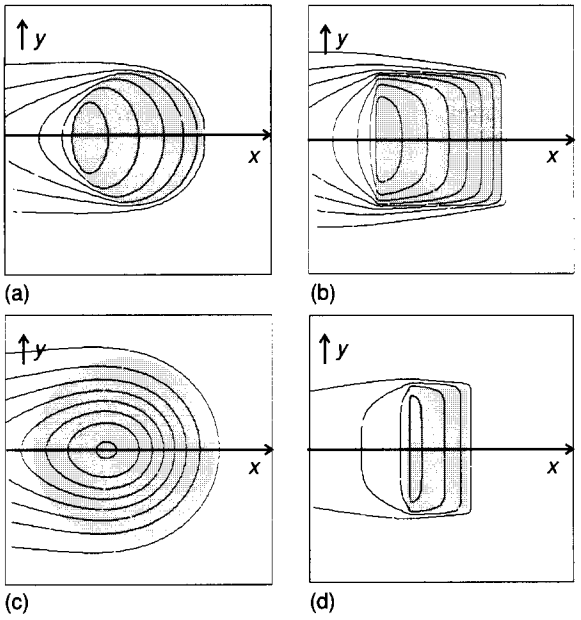

Figure 3 Isotherms ($z = 0$) induced by moving lasers with different spot geometries: (a) top hat, (b) square uniform, (c) Gaussian, (d) rectangular uniform $\phi = 1 : 2$.

4.3. Example

To illustrate the use of Fig. 4, the maximum surface temperature of C45, induced by a square laser spot (3 mm × 3 mm) with uniform power density, total absorbed power $P = 400\,\mathrm{W}$, and relative velocity $v = 10\,\mathrm{mm\,s^{-1}}$ is calculated. With the effective thermal diffusivity

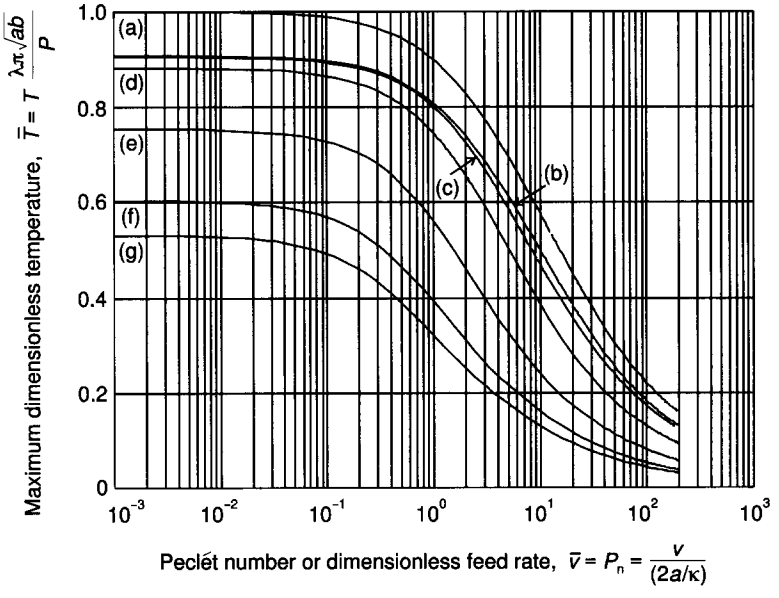

Figure 4 Maximum dimensionless surface temperature as a function of Peclét number for constant power P and constant a: (a) top hat, (b) Gaussian, (c) square, (d) rectangular $\phi = 1 : 2$, (e) rectangular $\phi = 1 : 5$, (f) rectangular $\phi = 1 : 10$, (g) rectangular $\phi = 1 : 15$.

$\kappa = 8.29 \times 10^{-6}\,\mathrm{m^2\,s^{-1}}$, the dimensionless speed $\bar{v}$ equals

$$\bar{v} = P_n \equiv \frac{2av}{\kappa} = \frac{2 \times \frac{1}{2}(3.0 \times 10^{-3}) \times 10^{-2}}{8.29 \times 10^{-6}} \approx 3.62$$

The dimensionless surface temperature $\bar{T}$ for $\bar{v} \equiv 3.62$ is read from Fig. 4 to equal $\bar{T} = 0.66$. With the effective thermal conductivity $\lambda = 48\,\mathrm{W\,m^{-1}\,K^{-1}}$, the actual increase in maximum surface temperature T is

$$T = \bar{T}\frac{P}{\lambda\pi\sqrt{ab}} = 0.66\frac{400}{48\pi[\frac{1}{2}(3 \times 10^{-3}) \times \frac{1}{2}(3 \times 10^{-3})]^{1/2}} \approx 1167$$

4.4. Approximating functions

The numerical results, obtained with the multi-integration multilevel algorithm, may be difficult to implement in a temperature control setup. Therefore, two simple functions which approximate the maximum surface temperature as a function of the velocity are presented.

4.4.1. Curve fit by splines

By dividing the total range of Peclét numbers as shown in Fig. 4 to n segments where $\bar{v}_{i,\mathrm{L}}$ and $\bar{v}_{i,\mathrm{U}}$ are the upper and lower boundary of the ith segment, the dimensionless temperature $\bar{T}_i$ in the ith segment is approximated by the cubic spline [10]

$$\bar{T}_i(\tau) = C_{i,0}(1-\tau)^3 + 3C_{i,1}(1-\tau)^2\tau + 3C_{i,2}(1-\tau)\tau^2 + C_{i,3}\tau^3$$

where $C_{i,j}$, $j = 0, \ldots, 3$ are constants, $\tau = [\log_{10}(\bar{v}) - \log_{10}(\bar{v}_{i,\mathrm{L}})]/[\log_{10}(\bar{v}_{i,\mathrm{U}}) - \log_{10}(\bar{v}_{i,\mathrm{L}})]$ and $\bar{v}_{i,\mathrm{U}} = \bar{v}_{i+1,\mathrm{L}}$. Constants $C_{i,j}$ have been calculated as to make the transition of the approximation from the ith segment to the $(i+1)$th segment continuous and smooth of the first order. This implies that $C_{i,3} = C_{i+1,0}$.

It was found that for the curves shown in Fig. 4 a good approximation is obtained when $n = 4$ with segments $\{0.004, \ldots, 0.4\}, \{0.4, \ldots, 4\}, \{4, \ldots, 40\}$ and $\{40, \ldots, 200\}$. In Table I the corresponding constants $C_{i,j}$ are listed and in Table II the approximation errors are listed.

A disadvantage of the spline approximation is that the relation between the process parameters and the surface temperature is lost. Therefore another (analytical) approximation is presented.

4.4.2. Approximation by combination of solutions

The literature available on analytical heat models due to laser beams either discuss point or line

TABLE I Spline coefficients $C_{i,j}$: 1 = top hat; 2 = Gauss; 3 = square; 4 = rectangular, $\Phi = 1{:}2$; 5 = rectangular, $\Phi = 1{:}5$; 6 = rectangular, $\Phi = 1{:}10$; 7 = rectangular, $\Phi = 1{:}15$

	$C_{1,0}$	$C_{1,1}$	$C_{1,2}$	$C_{1,3}$	$C_{2,1}$	$C_{2,2}$	$C_{2,3}$	$C_{3,1}$	$C_{3,2}$	$C_{3,3}$	$C_{4,1}$	$C_{4,2}$	$C_{4,3}$
1	1.000	0.999	1.016	0.955	0.922	0.851	0.733	0.612	0.455	0.338	0.259	0.198	0.157
2	0.906	0.902	0.923	0.859	0.825	0.748	0.625	0.410	0.358	0.264	0.201	0.156	0.123
3	0.909	0.906	0.925	0.864	0.831	0.760	0.648	0.535	0.387	0.283	0.213	0.164	0.129
4	0.883	0.878	0.903	0.820	0.774	0.677	0.544	0.410	0.280	0.203	0.151	0.117	0.092
5	0.754	0.747	0.770	0.660	0.583	0.471	0.356	0.255	0.173	0.125	0.094	0.072	0.056
6	0.602	0.599	0.615	0.487	0.412	0.306	0.235	0.171	0.115	0.082	0.061	0.047	0.037
7	0.531	0.527	0.540	0.410	0.336	0.253	0.192	0.136	0.093	0.067	0.050	0.038	0.030

TABLE II Approximation errors

Laser spot	Maximum error (%)	
	Spline	Analytical
Top hat	0.52	2.30
Gauss	0.74	2.23
Square	0.42	6.24
rectangular $\Phi = 1:2$	1.5	7.33
rectangular $\Phi = 1:5$	3.0	3.93
rectangular $\Phi = 1:10$	1.8	9.37
rectangular $\Phi = 1:15$	2.6	10.55

sources [14, 15], which are of limited use in surface processing, or are based on a modification of a Gaussian source [16, 17]. The latter model introduces a virtual displacement of the Gaussian beam in the z-direction above the actual surface to avoid infinite temperatures at the surface where the beam impinges. Arbitrary sources can be approximated by a suitable arrangement of Gaussian beams [19]. Additional (iterative) calculations are required to obtain the suitable value of the virtual z-displacement of the beam. From this profile the maximum temperature can be calculated [19].

A more simple approximation $\tilde{T}(v)$ of the maximum surface temperature $T(v)$ caused by a moving laser beam can be found by combining the asymptotic solutions T_s caused by a stationary beam and the temperature $T_f(v)$ caused by a fast moving beam according to the rule [11]

$$\frac{1}{\tilde{T}(v)^2} = \frac{1}{T_s^2} + \frac{1}{T_f(v)^2} \Rightarrow \tilde{T}(v) = \frac{T_s T_f(v)}{\sqrt{T_s^2 + T_f^2(v)}} \tag{11}$$

For the laser spot geometries discussed in this paper, the temperatures T_s for the stationary beams are listed in Section 3.

When the velocity of the semi-infinite metal, moving past the laser beam, becomes infinite, the heat flow in the metal becomes one-dimensional. The heat is only flowing in the direction perpendicular to the surface of the body. The corresponding surface temperature profile induced by an arbitrary shaped laser spot with intensity $I(x, y)$ equals [12]

$$T(x,y)|_{v\to\infty} = \frac{\sqrt{\kappa}}{\lambda\sqrt{\pi v}} \int_{x_0(y)}^{\min\{x,x_1(y)\}} \frac{I(\xi,y)}{\sqrt{x-\xi}}\, \mathrm{d}\xi \tag{12}$$

where $x_0(y)$ and $x_1(y)$ represent the left and right boundaries of the laser spot, respectively; for arbitrary laser spots these boundaries depend on the y value. Equation 12 is valid for high velocities where the effect of conduction in the metal in the processing direction is small compared to the convective effects due to the motion. That is, when $2av/\kappa > 10$.

Because the laser spots considered in this paper are supposed to be symmetric with respect to the x-axis, the maximum surface temperature $T_f(v)$ for high velocities is obtained for $y = 0$. Hence, this temperature can be calculated from

$$T_f(v) = \frac{\sqrt{\kappa}}{\lambda\sqrt{\pi v}} \max\left\{ \int_{x_0(y=0)}^{\min\{x,x_1(y=0)\}} \frac{I(\xi,0)}{\sqrt{x-\xi}}\, \mathrm{d}\xi \right\} \tag{13}$$

For a top hat power density, this high-velocity term equals

$$T_{\mathrm{f,TH}}(v) = \frac{2\sqrt{2}}{\lambda(\pi R)^{3/2}} P\sqrt{\frac{\kappa}{v}} \tag{14}$$

The maximum surface temperature $\tilde{T}_{\mathrm{H}}(v)$ for arbitrary velocity follows from (11) as

$$\tilde{T}_{\mathrm{TH}}(v) = \frac{2}{\lambda\pi R} P\sqrt{\frac{\kappa}{4\kappa + \frac{1}{2}\pi R v}} \tag{15}$$

For a Gaussian power density, the high-velocity term equals

$$T_{\mathrm{f,G}}(v) = \frac{c_1}{\lambda(\pi R_1)^{3/2}} P\sqrt{\frac{\kappa}{v}} \tag{16}$$

where

$$c_1 = \max_{x\in\{-1,1\}} \int_{-\infty}^{x} (\mathrm{e}^{-\xi^2}/\sqrt{x-\xi})\,\mathrm{d}\xi \approx 2.152$$

The maximum surface temperature $\tilde{T}_{\mathrm{G}}(v)$ for arbitrary velocity follows from (11) as

$$\tilde{T}_{\mathrm{G}}(v) = \frac{c_1}{\lambda R_1\sqrt{\pi}} P\sqrt{\frac{\kappa}{\pi^2 R_1 v + 4\kappa c_1^2}} \tag{17}$$

For a rectangular spot with width l, the high-velocity term equals

$$T_{\mathrm{f,R}}(v) = \frac{2}{\lambda b\sqrt{\pi l}} P\sqrt{\frac{\kappa}{v}} \tag{18}$$

The maximum surface temperature $\tilde{T}_{\mathrm{R}}(v)$ for arbitrary velocity follows from (11) as

$$\tilde{T}_{\mathrm{R}}(v) = \frac{2[l\sinh^{-1}(b/l) + b\sinh^{-1}(l/b)]}{\lambda b\sqrt{\pi l}} P\left(\frac{\kappa}{[l\sinh^{-1}(b/l) + b\sinh^{-1}(l/b)]^2 v + 4\pi\kappa l}\right) \tag{19}$$

The same results were obtained by Jaeger [13] based on another derivation. Equations 14 to 19 can be used to predict microstructural characteristics of the generated heat-affected zone [1, 5, 16–19]. In Table II the approximation errors of the dimensionless equivalents of Equations 15, 17 and 19 are listed. These errors are smaller than experimental errors in measuring quantities such as absorbed power or beam radius.

5. Experimental results

To validate the numerical results and the curve fits, experiments were performed on sandblasted C45 using a 1.7-kW continuous-wave CO_2 laser and integrating optics, yielding a square laser spot with uniform intensity up to $2.5 \times 10^8\ \mathrm{W\,m^{-2}}$.

The surface temperature was measured using a pyrometer. The experimental results are listed in Table III. They were checked and shown to be consistent with the numerical results of Fig. 4 within the accuracy of the experimental setup.

6. Conclusions

The surface temperature profile induced by moving laser beams can be obtained efficiently by

TABLE III Measured powers and temperatures

Spot size (mm × mm)	Velocity ($mm\,s^{-1}$)	P (W)	T (°C)
4.1 × 4.1	1	251.5	1218.25
4.1 × 4.1	1	496.9	1233.62
2.73 × 2.73	10	406.1	1400.78
2.73 × 2.73	10	408.8	1410.29
2.73 × 2.73	10	355.8	1482.60
2.73 × 2.73	10	384.0	1451.39
2.73 × 2.73	25	826.3	1225.93
2.73 × 2.73	25	1094.1	1251.67
2.73 × 2.73	50	780.5	1122.85
2.73 × 2.73	50	603.1	1118.82
2.73 × 2.73	50	587.7	1103.77

the use of the multilevel multi-integration algorithm. The maximum surface temperature as a function of the velocity has been calculated in dimensionless variables for several typical laser spot intensities.

For a laser surface temperature control setup, the spline or asymptotic approximation is more appropriate. Although the latter is less accurate, the influence of material parameters and processing conditions can be easily deduced.

References

1. C. J. HEUVELMAN, W. KÖNIG, H. K. TÖNSHOFF, J. MEIJER, P. K. KIRNER, M. RUND, M. F. SCHNEIDER and I. VAN SPRANG, *Ann. CIRP* **41**(2) (1992) 657.
2. J. MEIJER and I. VAN SPRANG, *Ann. CIRP* **40**(1) (1991) 1183.
3. M. BASS, *Encyclopedia of Physical Science and Technology* **7** (1987) 129.
4. A. BRANDT and A. A. LUBRECHT, *J. Comp. Phys.* **2** (1990) 348.
5. R. B. KUILBOER, P. K. KIRNER, J. MEIJER, M. RUND and M. F. SCHNEIDER, *Ann. CIRP* **43**(2) (1994) 585.
6. Th. RUDLAFF and F. DAUSINGER, *Proceedings of the 3rd Conference on Laser Treatment of Materials*, Erlangen, 1990, vol. 1, p. 251.
7. H. S. CARSLAW and J. C. JAEGER, *Conduction of Heat in Solids* (Clarendon Press, Oxford, 1959).
8. J. F. READY, *Effects of High-power Laser Radiation* (Academic Press, New York, 1971).
9. J. BOS and H. MOES, *Proceedings of the 20th Leeds-Lyon Symposium on Tribology*, 1994, p. 491.
10. C. DE BOOR, *A Practical Guide to Splines* (Springer-Verlag, Heidelberg, 1978).
11. J. A. GREENWOOD, *Wear* **150** (1991) 153.
12. H. BLOK, *Inst. Mech. Engrs., Proceedings of the General Discussion on Lubrication and Lubricants* **2** (1937) 222.
13. J. C. JAEGER, *J. Proc. R. Soc. NSW* **76** (1943) 203.
14. D. T. SWIFT-HOOK and A. E. F. GICK, *Welding J.* **52** (1973) 492.
15. D. ROSENTHAL, *Welding J.* **20** (1941) 220.
16. M. F. ASHBY and K. E. EASTERLING, *Acta Metall.* **32** (1984) 1935.
17. M. F. ASHBY and K. E. EASTERLING, *Acta Metall.* **30** (1982) 1969.
18. J. C. ION, K. E. EASTERLING and M. F. ASHBY, *Acta Metall.* **32** (1984) 1949.
19. H. R. SHERCLIFF and M. F. ASHBY, *Metall. Trans.* **22A** (1991) 2459.